Compliant Capacitive Wrist Sensor for Use in Industrial Robots

REINOUD F. WOLFFENBUTTEL, MEMBER, IEEE, KAMAL M. MAHMOUD, AND PAUL P. L. REGTIEN, MEMBER, IEEE

Abstract—**A sensor which is designed to measure the bending moments in the x and y directions, the force in the z direction and the torsion moment around the z direction is described. The sensor consists of two opposite electrode patterns with an elastomeric material in between, and electrical contacts to only the arm-side electrode pattern. Upon applying a force, the compliant intermediate will deform, causing a change in the separation and overlap between the electrodes, which results in a change in the capacitance. There are four sensitive capacitance patterns between the two electrodes. By combining the information from these four patterns it is possible to unambiguously distinguish between the three moments. Such a sensor can be used to improve the assembling performance of an industrial robot as the vision system might be obscured by the object to be manipulated at the moment the gripper establishes mechanical contact. The versatility of the sensor is demonstrated using an experiment, where a contour is tracked with constant contact force.**

I. INTRODUCTION

THE most demanding requirements imposed upon industrial assembly robots from the sensor point-of-view are contour tracking and assembly [1]–[5]. Up to now the contour tracking and object identification are mainly performed optically. Tactile sensing has widely been recognized to be an indispensable supplement to vision in such tasks. Tactile sensors can be used especially in cases where the manipulation arm might obscure the object to be handled at a crucial stage of its assembly. An effective tactile sensing is based on the combined operation of two types of tactile sensors. The first type is a directional wrist force sensor for detecting the force on the gripper when it meets a mechanical resistance. The second is a tactile imaging sensor that should be placed on the fingertip of the gripper. The wrist sensor is intended for course sensing and the tactile imaging sensor can be used to identify the shape of the object and to determine whether the object is properly positioned in the gripper, so that no slipping will occur. A robot wrist sensor will be presented that enables the measurement of the torques in the robot wrist in order to detect proper grasping and to avoid bumping into other objects during manipulation and assembly. Tactile sensing is not hampered by problems associated with object illumination and shadows. Therefore the vision system can be used for operations such as sizing, coarse orientation, etc., and the final stage of the object manipulation can be performed by the combined operation of a tactile imaging sensor and a wrist sensor, as shown in Fig. 1(a).

A robot wrist sensor can be built up of either force transducers or displacement transducers. In force type transducers the deformation of the force-sensing part is negligible, due to the large modulus of elasticity. Examples of the force-type sensor are the transducers based on strain-gauges or those that are based on piezoelectricity. The displacement-type transducer has a compliant sensor body. When a force is applied, the elastic sensor material is deformed. The resulting deformation is a measure of the applied force. The sensor discussed in this paper is a displacement-type tactile transducer.

The stiffness of the present-day robots, necessary for obtaining a high repeatability, produces considerable problems for assembly operations based on force information. Without compliance in the force control loop, either a very accurate positioning system or a very fast response is required in order to avoid undesirable situations such as jamming. A detailed analysis of the peg-in-hole problem shows that a suitable compliance in the force feedback loop can be used to avoid ambiguous situations [2] and automatic correction motions can be generated [3]. Fig. 1 shows the case of a peg-in-hole. When the peg completely misses the hole, a force F_Z will be detected, as shown in Fig. 1(b). This information can be used to suspend the intended insertion until the proper lateral position has been reached. When the tip of the peg is pressed against the chamfer, as shown in Fig. 1(c), this will cause a bending moment M_X and/or M_Y. Therefore, these two moments can be used to servo-control the lateral movements. The M_X and M_Y signals are, therefore, used for lateral fine-positioning. At zero values the hole is found. This paper discusses a compliant wrist sensor rather than the conventional force wrist sensors, which are based on strain gauges with active compliance [4], [5].

The compliant force/torque capacitive wrist sensor has been designed to measure the bending moments M_X and M_Y, in the x and y directions, respectively, the force F_Z, in the z direction and the torsion moment M_Z, around the z direction. The other forces in the gripper or the end-effector are incorporated in the respective moments in the wrist. A force in the x direction at the fingertip of the

Manuscript received February 14, 1990; revised June 30, 1990.

The authors are with the Department of Electrical Engineering, Laboratory for Electronic Instrumentation, Delft University of Technology, 2628 CD Delft, The Netherlands.

IEEE Log Number 9038900.

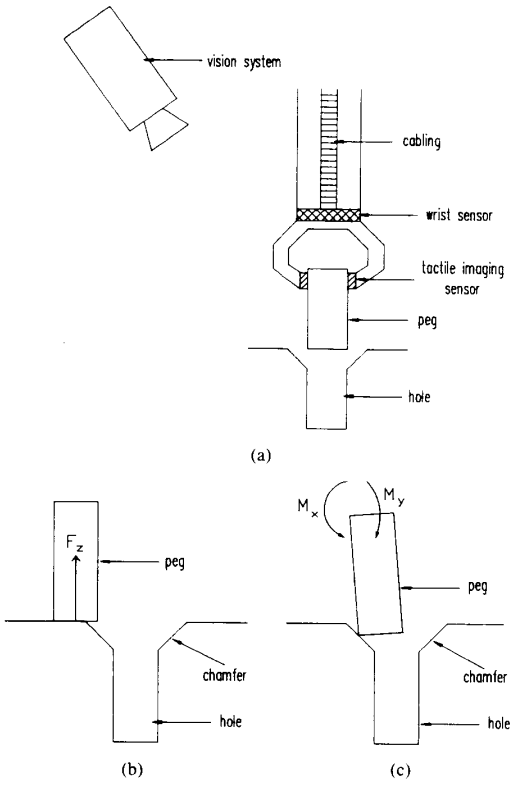

Fig. 1. (a) The positions of the vision, tactile, and wrist sensors in an industrial robot. (b) A situation where the peg completely misses the hole. (c) The peg is pressed against the chamfer.

industrial robot will result in a momentum M_X, in the wrist. Therefore, this sensor can be used in a 6 degree-of-freedom manipulator.

The sensor consists of two opposite electrode patterns with an elastomeric material in between, as shown in Fig. 2. The compliant intermediate will deform upon an applied force, causing a change in the separation and overlap between the electrodes and resulting in a capacitance change. For acceptable linearity, the relative change of the geometrical dimensions of the electrode to applied forces should be small. Moreover, the rigidity of the elastomer should be sufficiently high to allow the bending due to the weight of the gripper and the nominal load to be disregarded. Therefore, the change in capacitance is very small. The output signal of the sensor is processed using a very sensitive readout method [6], which involves a phase readout of an ac-operated charge amplifier with compensation of the nominal capacitance using a sine-wave voltage slightly less than 180 degrees out of phase with the driving voltage.

Important properties of sensors and actuators in the robot extremities are weight and the amount of cabling required for power and data transfer. The weight includes the servo motors of both wrist and fingers, the cables required for the tactile sensors and the proximity sensors. This sensor offers a reduction in weight and the amount

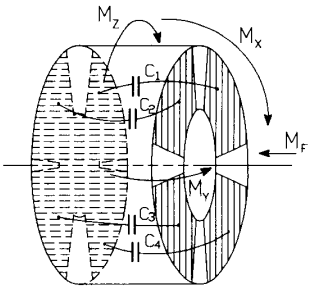

Fig. 2. The two electrode patterns and the capacitances between them.

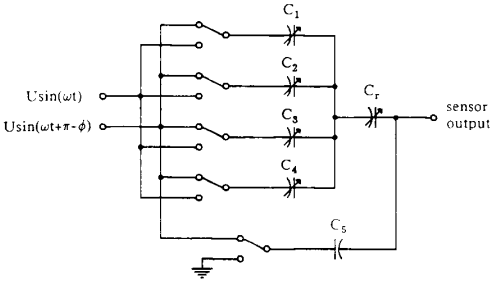

Fig. 3. The multiplexing circuit.

of wiring required, due to its simplicity of construction compared to other sensors using strain gauges [4], [5], [7], inductive elements [8], or a different structure with capacitive elements [9]. The reduction in the amount of wiring is achieved by using only four sensitive elements for independent detection of the three moments, by combining the information of these elements using on-sensor switching of the driving voltages and one-sided electrical connections. The multiplexing of the information from the four elements is accomplished as shown in Fig. 3. In this circuit, each of the four capacitors is switched either to the driving voltage $U \sin(\omega t)$ or to the compensating voltage $U \sin(\omega t + \pi - \phi)$.

As the sensor sensitivity is directly proportional to the nominal capacitance and the electrode area, an attempt has been made to reduce the number of electrode patterns that are needed for determining the force and moments, in order to maximize their area at constant total sensor area. This sensor can be used for many applications, for example in contour tracking and peg-in-hole insertion. In this paper, the sensor structure and the theoretical background will be considered, followed by the measured performance. Finally, the operation in a practical contour tracking system will be discussed.

II. Sensor Structure

The sensor consists of two opposite electrode patterns as shown in Fig. 4(a) and (b). Fig. 4(c) shows the electrodes as they are situated with respect to each other and Fig. 4(d) shows the equivalent capacitances between the electrodes. The sensor is realized on 7 cm diameter printed circuit boards. The nominal separation between the electrodes is determined by the thickness of the slab of natural

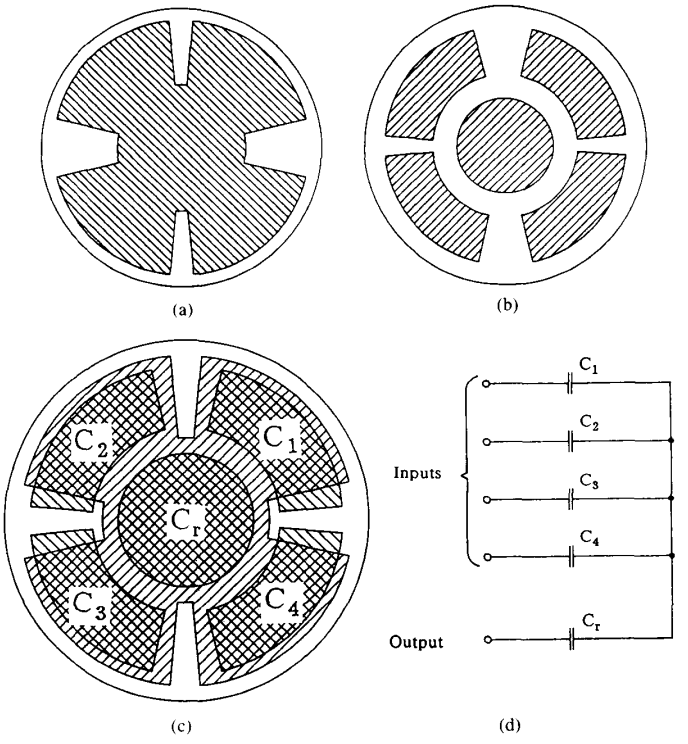

Fig. 4. (a), (b) The two electrode patterns. (c) The two electrodes as situated in respect to each other. (d) The equivalent capacitances between the electrodes.

rubber used and is 6 mm. Each of the four capacitive elements, C_1 through C_4, in Fig. 4(c) has an area of about 320 mm^2, and a nominal capacitance of about 1.4 pF (the relative permittivity of rubber is between 3 and 3.5). If a maximum change in thickness of about 10% is assumed, the maximum change in capacitance, per element, is 140 fF.

The four capacitors C_1 to C_4 are used in four different combinations to measure the four quantities of interest. The capacitor C_r is required for return coupling of the sensor signal to the electrode with the electrical connection to the readout circuits. By using this capacitor, all the electrical contacts to the sensor can be made at one side. The value of C_r should be large compared to the change in the other four capacitors. The value of C_r is independent of the moments. The maximum change due to F_Z is less than 10%. This change causes a nonlinearity in the output, which can be corrected for.

When disregarding fringing fields, the capacitance of any of the four capacitors as function of the three moment components and the force can be expressed as:

$$C = \int_{R_1}^{R_2} \int_{\theta_1}^{\theta_2} \cdot \frac{\epsilon_0 \epsilon_r r}{d_0 \pm \beta F_z \pm \alpha M_X r \sin(\theta) \pm \alpha M_Y r \cos(\theta)} \, dr \, d\theta \quad (1)$$

where

- R_1, R_2 inner and outer radii of the electrodes, respectively, refer to Fig. 5(a),
- θ_1, θ_2 angles by which one electrode pattern is enclosed,
- ϵ_0 permittivity of free space,
- ϵ_r relative permittivity of the elastomer,
- d_0 nominal separation between the electrodes,
- α, β sensitivity factors and depend on the elastic properties and the geometry of the rubber.

Only the torsion moment M_Z, does not directly appear in (1). This moment changes the limits of the integration interval θ_1 and θ_2. Equation (1) is difficult to solve analytically, therefore, a few approximations are introduced. In the following, we will discuss the change in one of the capacitors C_1 to C_4 in response to the change of each of the four measurands individually, and then the sensitivity of the sensor to each measurand will be derived.

First, consider the force F_Z. If only the force F_Z is applied and the other three moment components are zero, the capacitance given by (1) after integration gives

$$C = \frac{\epsilon_0 \epsilon_r (R_2^2 - R_1^2)(\theta_2 - \theta_1)}{2(d_0 \pm \Delta d_F)} = C_0 \frac{d_0}{d_0 \pm \Delta d_F} \quad (2)$$

where Δd_F is the physical change in the separation between the plates, which is represented by the term βF_Z in

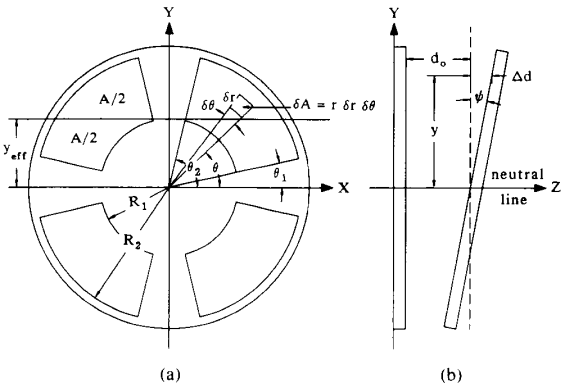

Fig. 5. (a) The effective capacitance area and the line dividing the electrode area into two equal parts and distance y_{eff} from the x–z plane. (b) One electrode is rotated with the angle ψ with respect to the other due to a bending moment.

(1). If $\Delta d_F \ll d_0$, the change in capacitance can be approximated as

$$\Delta C_F \approx C_0 \frac{\Delta d_F}{d_0} \approx \frac{C_0}{A_r Y} F_Z \tag{3}$$

where Y denotes the Young's modulus and A_r is the cross-sectional area of the rubber.

The total change in capacitance of the sensor for the force F_Z will be

$$\Delta C = (C_1 + C_2 + C_3 + C_4) - 4C_0 = \frac{4C_0}{A_r Y} F_Z \tag{4}$$

and the differential sensitivity of the sensor to the force will, therefore, be

$$\frac{\partial[(C_1 + C_2 + C_3 + C_4) - 4C_0]}{\partial F_Z} = \frac{4C_0}{A_r Y}. \tag{5}$$

The capacitance change is not affected by the three moments, because there is a cancellation due to the symmetry. For example, M_X will cause C_3 and C_4 to increase and C_1 and C_2 to decrease with the same amount. Therefore, the sum $C_1 + C_2 + C_3 + C_4$ is independent of M_X. A similar reasoning holds for the other two moments. For $C_0 = 1.4$ pF, $A_r = \pi R_r^2$, $R_r = 23$ mm, and $Y \simeq 10$ MN $\cdot$ m^{-2}, the sensitivity has a value of about 0.33 fF/N. A sensitivity of the capacitance change to phase angle conversion of 1.5°/fF results in a sensitivity for the force of about 0.5°/N. The sensitivity indicates the sensor response in the case of frontal touch with an object and greatly determines the collision response. For example, in the peg-in-hole problem, when the peg completely misses the hole, this would be detected as a force F_Z.

When a moment M_X is applied as shown in Fig. 2, one plate will rotate with respect to the other with the angle ψ, (Fig. 5(b)). Therefore, C_1 and C_2 will decrease due to the increase in the separation between the electrodes, while C_3 and C_4 will increase due to the decrease in the separation between the electrodes. For $\psi \neq 0$, the change in distance Δd between the electrodes is a function of the distance y. An average value y_{eff} is used, as approximation, which is equal to the change in the separation between the plates at the line parallel to the x–z plane and dividing the electrode area into two equal parts, as shown in Fig. 5(a). We will denote this value by Δd_m. This value is also a function of the angle ψ, but this dependence can be disregarded for small values of ψ.

The change in the capacitance due to the moment M_X can be approximated as

$$\Delta C_m \approx \pm C_0 \frac{\Delta d_m}{d_0} \approx \frac{4C_0 y_{eff}}{\pi Y R_r^4} M_X \tag{6}$$

where R_r is the radius of the rubber and y_{eff} is as indicated in Fig. 5(a). In the derivation of (6) pure bending is assumed.

The total change in capacitance of the sensor for the moment M_X is

$$(C_3 + C_4) - (C_1 + C_2) = 4\Delta C_m \tag{7}$$

and the differential sensitivity of the sensor to M_X is

$$\frac{\partial[(C_3 + C_4) - (C_1 + C_2)]}{\partial M_X} = \frac{16C_0 y_{eff}}{\pi Y R_r^4}. \tag{8}$$

This expression shows that the sensitivity is a function of the nominal capacitance and the properties and geometry of the elastic material. The sensitivity to M_X is not affected by the other two moments, because their effects will be canceled due to the symmetry, as explained above in the case of F_Z. From (8), the values of the constants stated above and $y_{eff} = 17$ mm, the sensitivity to M_X equals 43 fF/Nm. Inserting the sensitivity of 1.5°/fF of the readout circuit gives 65°/Nm.

With respect to the moment M_Y, all the equations above for M_X are valid, with the appropriate modifications, and the differential sensitivity to M_Y is given by

$$\frac{\partial[(C_1 + C_4) - (C_2 + C_3)]}{\partial M_Y} = \frac{16C_0 x_{eff}}{\pi Y R_r^4}. \tag{9}$$

The sensitivities to M_X and M_Y can be used to control the robot arm in the lateral movements. In the case of a hole with a chamfer, the force exerted by the chamfer on the peg tip is measured as M_X and/or M_Y in the wrist, and can be used to servo-control the gripper to perform the assembly.

To be able to measure the torsion moment M_Z, the electrodes are made in such a way that for a positive moment, the areas of C_1 and C_3 will increase while those of C_2 and C_4 will decrease, and vice versa (Fig. 4(c)). The change in any of the four capacitors C_1 to C_4 with respect to the torsion moment M_Z due to the change in the area of overlap is equal to

$$\Delta C_\theta = C_0 \frac{\Delta\theta}{\theta_2 - \theta_1} = \frac{2C_0 d_0}{\pi G R_r^4 (\theta_2 - \theta_1)} M_Z = \frac{\epsilon_0 \epsilon_r (R_2^2 - R_1^2)}{\pi G R_r^4} \tag{10}$$

where G is the shear-modulus of elasticity of the elastomer.

The total change in capacitance of the sensor structure for M_Z can be written as

$$(C_1 + C_3) - (C_2 + C_4) = 4\Delta C_\theta = \frac{4\epsilon_0\epsilon_r(R_2^2 - R_1^2)}{\pi G R_r^4} M_Z \qquad (11)$$

and the differential sensitivity will be

$$\frac{\partial[(C_1 + C_3) - (C_2 + C_4)]}{\partial M_Z} = \frac{4\epsilon_0\epsilon_r(R_2^2 - R_1^2)}{\pi G R_r^4}. \qquad (12)$$

In this case the sensitivity is directly proportional to $(R_2^2 - R_1^2)$ and inversely proportional to R_r^4 and G. For $Y = 10\ \mathrm{MNm}^{-2}$ and Poisson's ratio $\sigma = 0.3$, G is found from $G = Y/(2(1 + \sigma))$ to be equal to $3.8\ \mathrm{MN} \cdot \mathrm{m}^{-2}$. Thus, the sensitivity to M_Z is equal to 18 fF/Nm. Inserting the sensitivity of 1.5°/fF of the readout circuit gives 27°/Nm.

The practical readout circuit used for the capacitance-to-phase angle conversion is based on an ac-operated charge amplifier and is shown in Fig. 6(a) [6]. The output voltage U_0 satisfies

$$U_0 = -\frac{(C_{01} + \Delta C)}{C_t} U \sin(\omega t) + \frac{C_{02}}{aC_t} U \sin(\omega t). \qquad (13)$$

When $\Delta C = 0$ and $C_{02} = aC_{01}$, the output of this circuit is zero and shows a phase change of 180 degrees corresponding to undercompensation and overcompensation. The sensitivity to $\Delta C/C$ is equal to C_{01}/C_t, so the amplitude of the output voltage increases linearly with the relative change in capacitance. When the compensating signal with respect to the driving signal is not exactly π but $(\pi - \phi)$ out of phase, the phase change occurs gradually with the change in capacitance. The output amplitude will never be zero, which makes phase readout possible. Fig. 6(b) shows the charge amplifier using this technique. At the conditions $\omega R_t C_t >> 1$ and $C_{02} = aC_{01} = C_0$, the output voltage of this circuit can be described by

$$U_0 = -\frac{1}{C_t}\sqrt{\left(\Delta C + \frac{1}{2}\phi^2 C_0\right)^2 + (\phi C_0)^2} \cdot U \cos(\omega t - \theta) \qquad (14)$$

where

$$\theta = \arctan\left(\frac{0.5\phi^2 C_0 + \Delta C}{\phi C_0}\right). \qquad (15)$$

For allowing a phase detection at the output, the output voltage, U_0, should have a nonzero amplitude for all possible values of ΔC. From (14) it follows a minimum amplitude of $(\phi C_0 U)/C_t$ at $\Delta C = 0$.

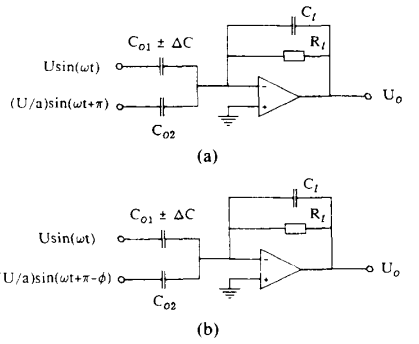

Fig. 6. The ac-operated charge amplifier. (a) Using a compensating signal π out of phase with the driving signal. (b) Using a compensating signal $\pi - \phi$ out of phase with the driving signal.

From (15) it can easily be verified that the differential phase sensitivity of θ for changes in capacitance will be equal to

$$\frac{\partial\theta}{\partial(\Delta C/C_0)} = \frac{1/\phi}{1 + [(\Delta C + C_0\phi^2/2)/\phi C_0]^2} \sim \frac{1}{\phi}. \qquad (16)$$

Thus the sensitivity is inversely proportional to the phase angle ϕ. It also appears that the nonlinearity increases with decreasing ϕ so a compromise should be made between sensitivity and nonlinearity. Selecting $\phi = 12°$ yields a sensitivity greater than 1.5°/fF and a nonlinearity less than 2%, making a reproducible detection of 0.4 fF possible [6]. As mentioned before, the maximum change in capacitance per element is 140 fF and the maximum change in capacitance in the sensor is 560 fF. Therefore, reproducible encoding into a 10-bit number is theoretically possible. However, the viscoelasticity of the rubber gives a hysteresis which strongly reduces the number of significant bits and in the practical sensor a 6-bit A/D conversion is implemented.

III. Measurements and Results

The sensor is realized on 7-cm diameter printed circuit boards. A natural rubber of 6-mm thickness is used as the compliant intermediate layer between the electrodes. The measurements are performed by applying the appropriate forces to a bar of well-determined length attached to one side of the sensor, while the other side is fixed. Each of the measurands is applied successively in time using standard weights and a known bar length. For each measurand the sensor is switched successively through all the modes of operation. The data in each of the four modes is read and recorded. From these data the sensitivities and cross-sensitivities can be derived. Fig. 7 shows the plots of the measured phase shift of the four modes as a function of the moment M_X. The output of M_X shows a hysteresis of about 6%, which makes the 6-bit AD conversion possible. This hysteresis is mainly due to the elastic properties of the rubber. From the figure, the sensitivity is about

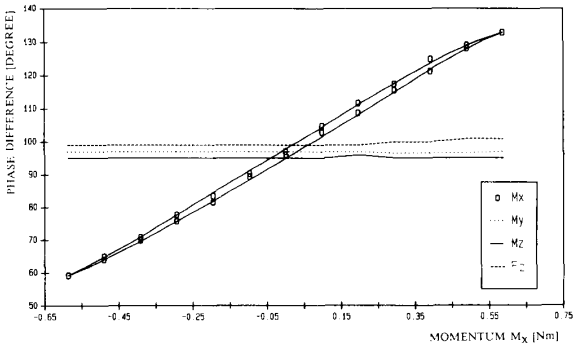

Fig. 7. The output phase difference for the four modes of operation versus the applied bending moment M_X.

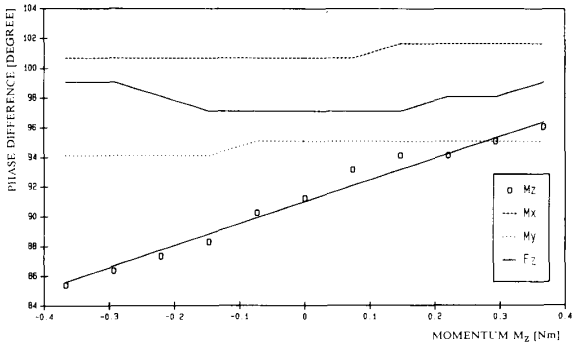

Fig. 8. The output phase difference for the four modes of operation versus the applied torsion moment M_Z.

$70°/N \cdot m$, which is in reasonable accordance with the theoretical value of $65°/N \cdot m$. The outputs of the other two moments and the force should be constant, but due to noise (from the power line and processor clock), the cross-sensitivity and errors in the experimental setup, the outputs are not completely constant. Because of the geometrical symmetry, the plots of the four modes as function M_Y will have a similar result to that of Fig. 7. Fig. 8 shows the output phase of the four modes versus M_Z. From the figure, the sensitivity for M_Z is about $14°/N \cdot m$, compared to the theoretical value of $27°/N \cdot m$. The output range and the sensitivity for M_Z are low compared to that of the bending moments. One of the reasons for the low sensitivity and limited output range is the higher torsional stiffness of the rubber compared to the lateral stiffness. There are fluctuations in output of the bending moments and force, for the same reasons as those for M_X. The sensitivity and the output range of M_Z can be improved by splitting each of the sensitive elements into two parts to increase the area of overlap due to the moment M_Z at the expense of the sensitivity to M_X and M_Y, as their electrode area will be reduced. Fig. 9 shows the phase outputs of the four modes versus the force F_Z. We see from the figure that the sensitivity to F_Z is low compared to that of M_X and M_Z, because of the small thickness of the elastic material. The measured sensitivity is about $0.4°/N$, which

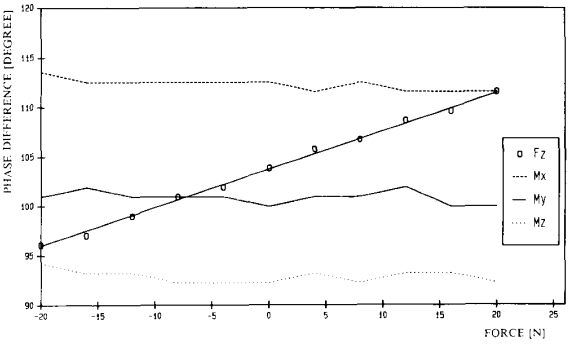

Fig. 9. The output phase difference for the four modes of operation versus the applied force F_Z.

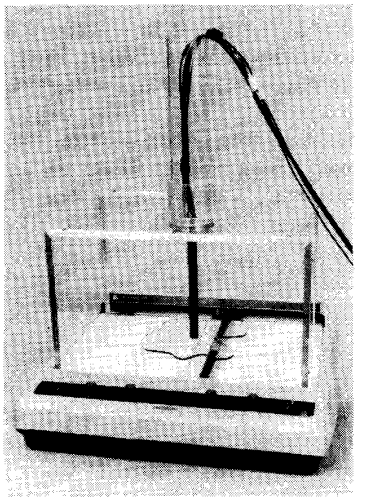

Fig. 10. Photograph of the sensor and the plotter used in the contour tracking experiment.

is in reasonable agreement with the theoretical value of $0.5°/N$. The other outputs should be constant, but for the same reasons as mentioned above, the three outputs show some fluctuations. There is an obvious cross-effect between F_Z and the moments. At an increasing F_Z the dielectric will be compressed resulting in a reduced electrode distance and an increased nominal capacitance for all electrodes. Therefore, the sensitivity for the torques will increase at increasing F_Z. This effect is not revealed by the measurements in Figs. 7–9, because measurands have been applied successively.

IV. Contour Tracking Experiment

Vision is often used for contour tracking in a welding robot. However, a tactile force/torque sensor may have a better performance in this application. As a test for the performance of this sensor in such an application, an experiment has been performed using M_X and M_Y to servo-control a pen of an x–y plotter to follow the contour of an object with a constant contact force. Fig. 10 shows a photograph of the plotter and the sensor. The sensor is fixed

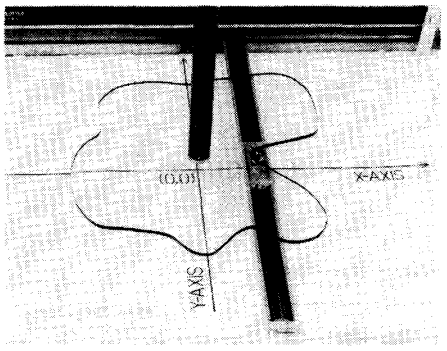

Fig. 11. Photograph of the object and the pen of the plotter.

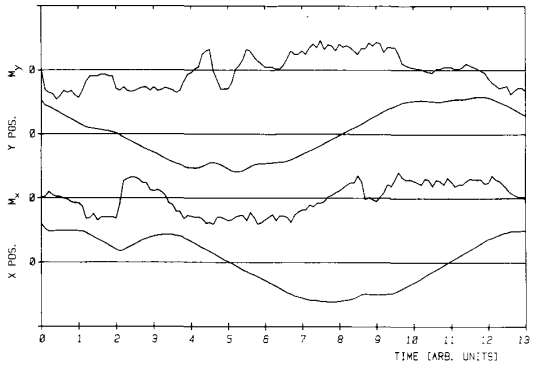

Fig. 12. A plot of the x and y position of the pen and M_X and M_Y on the sensor versus time.

between the rod and the frame which is attached to the plotter. Fig. 11 shows a close-up of the object and the pen, which is pressing against the edge of the object. Fig. 12 shows a plot of the x and y positions of the pen and the moments, M_X and M_Y, versus time for one complete cycle of the pen around the edge of the object. From the figure we see that the moment is proportional to the slope of the position, and that the direction of the movement changes when the absolute value of the corresponding momentum exceeds the preselected threshold value. At $t = 2$, the y-position is zero and the x-position curve shows a minimum. This point corresponds to the position at which the pen is touching the object in Fig. 11. At this point M_X turns from positive to negative. This experiment confirms the suitability of this type of force sensor for the contour tracking problem.

V. Conclusions

By using specially shaped electrode patterns in a simple two-layer capacitor, it is possible to separate the three moment components using symmetry in the electrode geometry. This prototype sensor shows a sensitivity better than $70°/N \cdot m$ with a cross sensitivity for the non-selected mode smaller than $0.1°/N \cdot m$. Some advantages of this sensor over the multibridges strain gauges type are: It does not require a complex construction, offering a reduction in weight. Since the sensor consists of only four sensitive elements, multiplexing of the signals from these elements reduces the amount of cabling required. The phase shift output can easily be converted into a digital signal by simple counters. It is possible to distinguish between the three moments by combining the information of the four patterns. The compliant intermediate makes the sensor inherently suitable for compliant peg-in-hole insertion and contour tracking with constant contact force.

Future research will involve the realization of a custom chip that contains all electronics required for the readout and the AD conversion based on pulsewidth modulation.

References

[1] R. F. Wolffenbuttel and P. P. L. Regtien, "Integrated tactile imager with an intrinsic contour detection option," *Sensors and Actuators*, vol. 16, pp. 141–153, 1989.

[2] S. Simunovic, "Force information in assembly process," in *Proc. 5th Int. Symp. on Ind. Robots*, pp. 415–431, 1975.

[3] H. Van Brussel and J. Simons, "The adaptable compliance concept and use for automatic assembly by active force feedback accommodations," in *Proc. 9th Int. Symp. on Ind. Robots*, pp. 167–181, Washington, DC, Mar. 1979.

[4] R. M. Inigo and R. M. Kossey, "Closed-loop control of a manipulator arm using a wrist force sensor," *IEEE Trans. Ind. Electron.*, vol. IE-34, pp. 371–378, Aug. 1987.

[5] H. Van Brussel and J. Simons, "Automatic assembly by active force feedback accommodation," in *Tactile & Non-Vision*, (Ed., A. Pugh). London, UK: IFS Ltd., pp. 53–66, 1986.

[6] R. F. Wolffenbuttel and P. P. L. Regtien, "Capacitance-to-phase angle conversion for the detection of extremely small capacitances," *IEEE Trans. Instrum. Meas.*, vol. IM-36, pp. 868–872, 1987.

[7] H. van Brussel, H. Belien and H. Thielemans, "Force sensing for advanced robot control," in *Proc. 5th Int. Conf. on Robot Vision and Sensory Controls*, pp. 59–68, 1985.

[8] G. Piller, "A compact six-degree-of-freedom force/torque sensor for assembly robots," in *Robot Sensors: Tactile & Non-Vision*, (Ed., A. Pugh), London, UK: pp. 67–74, 1986.

[9] A. H. Falkner, H. S. Sahotay, and M. Yeung, "Practical developments in robot sensing," in *Proc. 6th Int. Conf. on Systems Engineering*, pp. 851–858, 1988.